The importance of both fibroblasts and keratinocytes in a bilayered living cellular construct used in wound healing

Abigail M. Wojtowicz, PhD[1]; Steve Oliveira, MS[1]; Mark W. Carlson, PhD[1]; Agatha Zawadzka, MS[2]; Cecile F. Rousseau, PhD[2]; Dolores Baksh, PhD[1]

1. Research and Development Department,
2. Preclinical Department, Organogenesis, Inc., Canton, Massachusetts

ABSTRACT

Cross talk between fibroblasts and keratinocytes, which maintains skin homeostasis, is disrupted in chronic wounds. For venous leg ulcers and diabetic foot ulcers, a bilayered living cellular construct (BLCC), containing both fibroblasts and keratinocytes that participate in cross talk, is a safe and effective product in healing chronic wounds. To show the importance of both cell types in BLCC, constructs were generated containing only fibroblasts or only keratinocytes and compared directly to BLCC via histology, mechanical testing, gene/protein analysis, and angiogenesis assays. BLCC contained a fully differentiated epithelium and showed greater tensile strength compared with one-cell-type constructs, most likely due to formation of intact basement membrane and well-established stratum corneum in BLCC. Furthermore, expression of important wound healing genes, cytokines, and growth factors was modulated by the cells in BLCC compared with constructs containing only one cell type. Finally, conditioned medium from BLCC promoted greater endothelial network formation compared with media from one-cell-type constructs. Overall, this study characterized a commercially available wound healing product and showed that the presence of both fibroblasts and keratinocytes in BLCC contributed to epithelial stratification, greater tensile strength, modulation of cytokine and growth factor expression, and increased angiogenic properties compared with constructs containing fibroblasts or keratinocytes alone.

Normal cutaneous wound healing is a dynamic and complex process that can be summarized in the following phases: hemostasis, or formation of a fibrin clot, inflammation/granulation, reepithelialization, and contraction/tissue remodeling. These phases require integration of biological and molecular events, such as cellular proliferation, migration, cytokine and growth factor secretion, differentiation, and extracellular matrix production.[1–3] Failure to transition from one phase to the next causes an imbalance in the normal sequence of acute wound healing events, which can result in delayed healing and may lead to a chronic, nonhealing wound.[4,5]

Chronic wounds of the lower extremities afflict a significant proportion of the population in the United States. Venous leg ulcers (VLUs), for example, are estimated to account for 75% of all lower extremity ulcerations, and the annual prevalence of VLUs is 600,000.[6] Approximately 8.3% of the US population suffers from diabetes, and the annual incidence of diabetic foot ulcers (DFUs) in patients with diabetes is 2–6%, with a lifetime incidence as high as 25%.[7,8]

Fibroblasts and keratinocytes are two of the major cell types that respond to the inflammatory phase in the cutaneous repair/regeneration process. Inflammatory signals activate the proliferation and maturation of these two cells types, which is essential for wound healing.[2,9] Furthermore, keratinocytes and fibroblasts communicate with each other via double paracrine signaling loops, known as cross talk or dynamic reciprocity, which coordinate their actions to restore normal tissue homeostasis after wounding.[5,10] At the onset of acute wound healing, signaling from inflammatory cells at the wound site promotes fibroblast migration inward from the wound margins.[2] Fibroblasts secrete paracrine factors, such as basic fibroblast growth factor (bFGF/FGF-2),[5,9] keratinocyte growth factor (KGF/FGF-7),[1,3,11] vascular endothelial growth factor A (VEGF-A)[9] and insulin-like growth factor-1 (IGF-1),[12,13] which signal to adjacent keratinocytes. Furthermore, in response to paracrine signaling from keratinocytes and inflammatory cells, fibroblasts synthesize collagen and promote cross-linking to form an extracellular matrix, and differentiate into a myofibroblastic phenotype to facilitate wound closure.[1,5,9,14]

Keratinocytes recruit, stimulate, and coordinate the actions of multiple cell types involved in healing and recapitulate the epidermal barrier layer of the skin. In response to disruption of the barrier, keratinocytes release prestored interleukin 1 (IL-1), which acts as both an autocrine and paracrine signal that activates and increases keratinocyte migration and proliferation, as well as mobilizes surrounding cells to aid in healing.[9,10] IL-1 is one example of double paracrine signaling because it up-regulates fibroblast production of KGF, which in turn stimulates keratinocyte proliferation and migration.[15] Keratinocytes also secrete angiogenic growth factors, such as vascular endothelial growth factor (VEGF)[9] and platelet-derived growth factor (PDGF),[11] which induce endothelial cell migration and angiogenesis in the wound bed,[16] and, in the case of PDGF, promote fibroblast proliferation and production of extracellular matrix.[9] In normal skin, the growth factors and cytokines secreted by fibroblasts and

keratinocytes are important for maintaining tissue homeostasis, and in cutaneous wounds, this coordinated cross talk leads to the recruitment of cells necessary for complete wound closure.[10]

To take advantage of the wound healing attributes of keratinocytes and fibroblasts, bioengineered products that incorporate these cell types have been developed to treat chronic wounds. When applied to the wound site, the cells supply signaling molecules, growth factors, and extracellular matrix proteins that aid healing. Commercially available therapies include products that incorporate keratinocytes (e.g., EpiCel), fibroblasts (e.g., Dermagraft), or both keratinocytes and fibroblasts (e.g., Apligraf).[17]

The bilayered living cellular construct (BLCC, Apligraf, Organogenesis, Inc., Canton, MA) used in the current study contains keratinocytes and fibroblasts in a three-dimensional bovine collagen matrix, which promotes wound healing and has been shown in randomized, controlled clinical trials to reduce healing time and increase the incidence of complete wound closure in both DFUs and VLUs.[18,19] This manuscript provides characterization of this commercially available wound healing product. The aim of the current study was to evaluate the individual and synergistic contributions of fibroblasts and keratinocytes to the BLCC in terms of tissue morphology, mechanical strength, gene expression, cytokine/growth factor production, and angiogenic properties.

MATERIALS AND METHODS

Culture of human keratinocytes and dermal fibroblasts

Keratinocytes and dermal fibroblasts were derived from donated human neonatal foreskin tissue following informed consent procedures approved by the Institutional Review Boards at qualified tissue donation sites. Upon receipt, each tissue was enzymatically dissociated using a trypsin/collagenase solution, and the resulting cell suspension was expanded in monolayer culture to generate cell banks as described previously.[20] Keratinocytes and fibroblasts were derived from separate tissues, and selective culture conditions were used to promote the growth of either keratinocytes or fibroblasts within a single cell bank. Briefly, keratinocytes were cultured on dishes coated with bovine collagen type I (0.04 mg/mL coating concentration) and grown in calcium-free Dulbecco's modified Eagle's Medium (DMEM)/Ham's F-12 (proprietary blend) supplemented with 0.3% chelated bovine calf serum (cBCS). Fibroblasts were cultured in DMEM with high glucose and 10% bovine calf serum (BCS).[21] For the production of all constructs, fibroblasts were used at passage 6 and keratinocytes were used at passage 4.

Generation of BLCC, Fibroblast matrix, and Epithelium only constructs

The composition and construction of the BLCC has been described previously.[21] Briefly, the BLCC was fabricated in a 75 mm diameter polycarbonate transwell with 3.0 μm porosity, which enabled diffusion of the culture medium from the bottom of the construct while maintaining the top of the construct at an air–liquid interface to promote epithelial
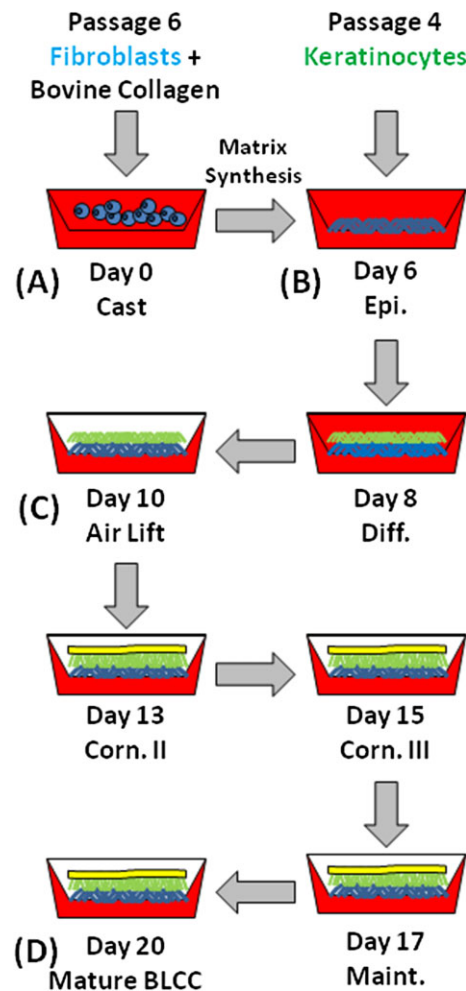

Figure 1. Outline of the BLCC manufacturing process. (A) The fibroblast layer is formed by the deposition of a fibroblast/collagen layer on Day 0, which is incubated for 6 days to promote matrix synthesis. (B) Keratinocytes are then seeded onto the surface of the fibroblast/collagen matrix and incubated from Day 6 to Day 10 with a media change at Day 8 to allow epidermal differentiation. (C) At Day 10 after cast, the constructs are brought to the air–liquid interface to induce cornification of the epidermal layer. (D) The mature construct is ready for use at Day 20. Time points specified in the figure correlate to media changes. The red background represents media and illustrates the air lift step in which constructs are fed only from the bottom starting at Day 10. Fibroblasts and matrix are represented in blue; keratinocytes/epithelium are represented in green; and the stratum corneum is represented in yellow. Epi indicates Epidermalization, Diff indicates Differentiation, Corn indicates Cornification, Maint indicates Maintenance. BLCC, bilayered living cellular construct.

development at later time points in the process. As outlined in Figure 1, the dermal layer was formed by the deposition of fibroblasts mixed with bovine collagen type I at Day 0 of construct generation. The initial seeding density of the fibroblasts in the collagen matrix is detailed in Parenteau

et al.[20] The fibroblast/collagen constructs were submerged in culture media consisting of DMEM/Ham's F-12 supplemented with 5% BCS and 0.05 mg/mL sodium ascorbate and incubated at 37 °C in 10% CO_2. At Day 6 after cast, a suspension of keratinocytes was seeded onto the surface of the fibroblast/collagen layer in DMEM/F-12 supplemented with 0.3% cBCS. The initial seeding density of the keratinocytes seeded on top of the collagen matrix is detailed in Parenteau et al.[20] The constructs were then cultured for 2 days to allow the keratinocytes to proliferate and migrate over the fibroblast/collagen layer. On Day 8, the medium was changed to DMEM/F-12 supplemented with 0.3% BCS, and 0.265 mg/mL calcium chloride (final concentration) was added to the media to promote differentiation of the keratinocytes. At Day 10, the constructs were brought to the air–liquid interface by adding a Cornification Medium consisting of DMEM/F-12 supplemented with 2% BCS and 0.05 mg/mL sodium ascorbate to only the bottom of the transwell to induce cornification of the epidermal layer. The Cornification Medium was refreshed on Days 13 and 15. Finally, on Day 17, the medium was changed to a Maintenance Medium consisting of DMEM/F-12 with 1% BCS, and the BLCC was allowed to mature up to Day 20. All experiments on the final construct were performed on Day 20.

The procedure used to generate the BLCC described above was modified to generate two experimental constructs. The "Fibroblast matrix" construct was comprised of the fibroblast/collagen layer but no keratinocytes were added. The "Epithelium only" construct was comprised of an acellular collagen layer, which was equivalent in volume to the fibroblast/collagen layer in the BLCC, and was seeded with keratinocytes as described above. Both of these experimental constructs were cultured to Day 20. Note that the "Fibroblast matrix" and "Epithelium only" groups were included in this work as experimental groups to evaluate the contributions that keratinocytes impart to the overall biological profile of the BLCC construct when in the presence of fibroblasts. Importantly, this work did not focus on the "Fibroblast matrix" and "Epithelium only" groups as potential product embodiments, but rather restricted the generation of these groups as major constituents of the BLCC construct.

Histological and immunohistochemical staining

Five-micrometer formalin-fixed and paraffin-embedded sections were stained with Harris Hematoxylin (Poly Scientific, Bay Shore, NY) & Eosin Y (Leica Microsystems, Buffalo Grove, IL) for evaluation of tissue morphology at Day 20. Mouse anti-human cytokeratin 1/10 (AbD Serotec, Raleigh, NC) was used to identify differentiated keratinocytes. Mouse anti-human collagen type IV (Novotec, Lyon, France) was used to characterize the basement membrane, and rabbit anti-human Ki67 (Vector Laboratories, Burlingame, CA) was used to identify proliferating cells. Tissue sections ($n = 3$ samples per group) were deparaffinized and hydrated in phosphate-buffered saline (PBS) solution at room temperature. After appropriate antigen retrieval, sections were incubated with the primary antibodies (diluted in PBS with 3% bovine serum albumin) against cytokeratin 1/10, collagen type IV, or Ki67. Endogenous peroxidase activity was blocked with 0.5% hydrogen peroxide. Tissues were then incubated with ImmPRESS rabbit or ImmPRESS mouse kits (Vector Laboratories) for 30 to 45 minutes at room temperature. Antigen–

antibody complexes were detected with tetrahydrochloride diaminobenzidine (Vector Laboratories), showing positive staining in dark brown. Sections were counter-stained using Mayer's hematoxylin solution (Electron Microscopy Sciences, Hatfield, PA). The sections were observed at 20× magnification, and digital pictures were recorded using a Zeiss microscope and AxioVision software (Carl Zeiss, Oberkochen, Germany).

Cell proliferation

BLCCs were generated as described above, with the addition of a single bromodeoxyuridine (BrdU) pulse during critical process steps to identify proliferating cells. Pulsing was performed by the addition of 10 nM BrdU (BD Biosciences, San Jose, CA) to the media approximately 12 hours prior to a scheduled media change. Each construct received only one BrdU pulse during the 20-day culture process, and three biological replicates were pulsed per time point. The time points investigated were Days 7, 9, 12, 14, and 16, which correspond to the media changes called Differentiation, Cornification I, Cornification II, Cornification III, and Maintenance, respectively, as outlined in Figure 1. At Day 20, BrdU staining was performed on paraffin sections using the BrdU in situ detection kit (BD Pharmingen, San Jose, CA), according to the manufacturer's instructions. Negative controls were included by staining BLCC ($n = 3$) that were not pulsed with BrdU. Sections were counterstained with hematoxylin, dehydrated with Clear-rite 3, and cover slipped. Quantification was performed by counting the number of BrdU-positive keratinocytes and fibroblasts in a single 24 mm biopsy sample processed histologically ($n = 3$ samples per time point). This total number was obtained by adding together the number of BrdU-positive keratinocytes and fibroblasts in 20 separate 1.2 mm wide images per 24 mm histology section.

Fibroblast viability and counts

The epithelial (keratinocyte) layer and fibroblast matrix of Day 20 BLCCs were physically separated using forceps. The fibroblast matrices were enzymatically digested in order to quantify the number of intact cells in the fibroblast matrix of the final BLCC (Day 20). Epithelial/keratinocyte layers were not included in this analysis because the cornified tissue formed in the stratified epithelium cannot reliably be digested using collagenase. Briefly, four BLCCs were removed from the transwell membrane, then the layers were separated using a pair of forceps, and the resulting fibroblast matrix layer was transferred to a collagenase solution (50% collagenase type I [Sigma Aldrich, St. Louis, MO], 2.5% trypsin, 0.75% glucose, 0.38% fungizone, 50 mg/mL gentamicin in 1× PBS) and incubated statically for approximately 1 hour at 37 °C in a water bath. After digestion, the samples were centrifuged and resuspended in DMEM +10% bovine calf serum. Trypan blue exclusion was used to quantify total cell number as well as the percentage of intact cells, which was used as an indication of cell viability.

Maximum tensile load

BLCC ($n = 3$), Fibroblast matrix ($n = 3$), and Epithelium only ($n = 3$) constructs were evaluated for maximum tensile load

using an Instron Materials Testing System (Model 3342, Instron, Canton, MA). The Fibroblast matrix constructs used in this arm of the study were cultured to Day 6 as this represents the point in the process where the matrix compartment has matured and is suitable for keratinocyte seeding. Briefly, uniaxial tension was applied to 12.5 mm × 50 mm rectangular strips cut from each construct. Manual screw-type grips were used to load the samples onto the tensile testing device, and elongation was conducted at a constant rate of 60 mm per minute until failure. During the test, samples were moistened with reverse osmosis deionized water for better attachment to the grips. A 10 N load cell was used to detect the maximum load that the samples could withstand before rupture. Statistical analyses were performed using a one-way analysis of variance (ANOVA).

RNA isolation and gene expression analysis

Eight-mm biopsy punches of the constructs were stored in Buffer RLT (Qiagen, Valencia, CA) at −20 °C. The biopsies were disrupted using a mortar and pestle, lysed, and homogenized prior to freezing. RNA was isolated using the Qiagen RNeasy RNA isolation kit, according to the manufacturer's instructions (Qiagen). The iScript cDNA Synthesis Kit (BIORAD, Hercules, CA) was used to convert the isolated RNA to cDNA according to the manufacturer's instructions. cDNA from biological replicates ($n = 3$ for BLCC and Fibroblast matrix; $n = 2$ for Epithelium only) was analyzed using the Human Growth Factor PCR array (SA Biosciences,Valencia, CA), which measures cDNA corresponding to 84 genes related to growth factors and and cytokines. Gene expression was analyzed relative to GAPDH and β-actin house-keeping genes using the ΔΔCt method. Cluster diagrams were generated with the constructs on the x-axis and genes on the y-axis using the dCHIP analysis software developed by Li and Wong.[22]

Cytokine and growth factor protein concentrations

Conditioned media were collected from Fibroblast matrix, Epithelium only, and BLCC at each media change throughout the culture process as outlined in Figure 1 (Days 6, 8, 10, 13, 15, 17, and 20; $n = 3$ constructs/time point) and stored at −20 °C until analysis. Cytokine and growth factor (IL-6, IL-8, VEGF) concentrations at each time point were measured using a multiplexed cytometric bead array (CBA, BD Biosciences) and a FACS Canto II flow cytometer (BD Biosciences). IGF-1 and BMP-2 concentrations in the conditioned media at sample maturity (Day 20) were measured via enzyme-linked immunosorbent assay (ELISA), according to the manufacturer's instructions (human IGF-1 and BMP-2 ELISA kits, R&D Systems, Minneapolis, MN).

Maintenance of endothelial networks

Conditioned media collected from the BLCC, Fibroblast matrix, and Epithelium only constructs at maturity (Day 20) were used as test articles in a modified in vitro angiogenesis assay. Human umbilical vein endothelial cells (hUVECs) (Lonza Walkersville) at passage 4 were fluorescently labeled with DiI (1,1′—dioctadecyl-3,3,3′,

3′-tetramethylindocarbocyanine perchlorate) (Invitrogen, Carlsbad, CA) following the protocol provided by the manufacturer. Briefly, trypsinized cells were washed once with PBS, resuspended in 1000× dilution of DiI dye in PBS, and incubated at 37 °C for 5 minutes followed by incubation at 4 °C for 15 minutes. Upon completion of the incubation steps, cells were washed with PBS and resuspended in culture medium (EBM-2, Lonza Walkersville). The fluorescently labeled hUVECs were seeded at 20,000 cells/cm² onto a fully gelled Matrigel basement membrane matrix (BD Biosciences) and incubated for 24 hours in fully supplemented endothelial growth medium (EGM-2) to promote network formation. After 24 hours, the cultures were replenished with conditioned media from the various experimental groups ($n = 3$ samples/group) and the extent of hUVEC network survival was monitored over 6 days using time-lapse microscopy. Time-lapse images were acquired at 5× magnification with a Zeiss microscope and AxioVision software and were submitted to Wimasis Image Analysis for quantification of network length, branching points, and loops using WimTube software (Wimais GmbH, Munich, Germany).

Statistical analysis

All statistical analysis were performed in SPSS Version 20 (IBM Corporation, Armonk, NY). For all data, Shapiro–Wilk and Levene statistics were applied a priori to verify normality and homogeneity of variances, respectively. Data which met the assumptions for one-way ANOVA were analyzed using ANOVA with post hoc Tukey methods. Nonnormal datasets were analyzed by Kruskal–Wallis using a post hoc pairwise comparison of mean ranks. Datasets that exhibited normality but did not exhibit homogeneity of variances were subjected to ANOVA with Welch's correction factor and post hoc Dunnet's T3. Groups were considered statistically different if $p < 0.05$. All data are presented as mean ± standard deviation unless otherwise indicated.

RESULTS

Histological construct characterization

Hematoxylin and eosin staining showed differences in epithelial development between the constructs (Figure 2A–C). Only the BLCC contained a fully differentiated epithelium with stratified layers and a stratum corneum. Differentiated keratinocytes were identified in the BLCC via positive staining for Cytokeratin 1/10, while the Epithelium only and Fibroblast matrix constructs did not contain Cytokeratin 1/10 (Figure 2D–F). Collagen type IV staining at the dermal–epidermal interface was observed in the BLCC only, confirming that both keratinocytes and fibroblasts are necessary for basement membrane deposition (Figure 2G–I).

Cell proliferation and viability

BrdU incorporation was used to identify proliferating cells during the construct manufacturing process. Staining for BrdU at different stages of BLCC development showed that the fibroblasts and keratinocytes were proliferating throughout the entire maturation process (Figure 3A–F). Quantification of
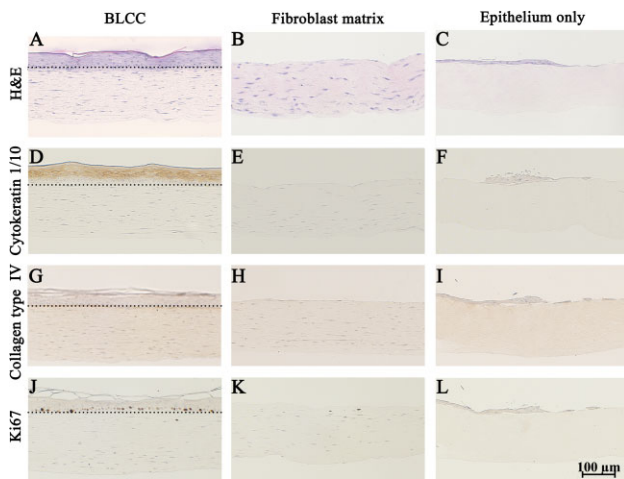
Figure 2. Histological and immunohistochemical staining shows differences between BLCC, Fibroblast matrix, and Epithelium only constructs. Hematoxylin and eosin (H&E) (A–C); Cytokeratin 1/10 (D–F); Collagen type IV (G–I); and Ki67 (J–L) show functional and morphological differences between constructs. Differentiated keratinocytes were only identified in the BLCC (D–F). Collagen type IV, indicating basement membrane deposition, and Ki67 immunostaining for proliferating cells were found at the interface of the dermal and epidermal layers in the BLCC, but not in Fibroblast matrix or Epithelium only constructs (G–I, J–L). Dotted lines in (A), (D), (G), and (J) demarcate the dermal–epidermal interface in the BLCC. Day 20 results shown. Each image is representative of $n = 3$ samples per group. BLCC, bilayered living cellular construct.

BrdU-positive cells showed that the number of proliferating keratinocytes was relatively high at Days 7 and 16 and decreased from Days 9 to 14 (Figure 3G). The BrdU spike at Day 7 corresponds to the Differentiation stage, in which basal keratinocytes proliferate to form the suprabasal layers of the epithelium. Days 9–14 correspond to the Cornification stage, which involves terminal differentiation of the suprabasal cells resulting in a cornified epithelium. Day 16 corresponds to the Maintenance stage at which time the cornified epithelium has formed and stem/transit amplifying cells continue to divide, replenishing keratinocyte layers in the epidermis as the upper layers of the epidermis undergo cell death to thicken the stratum corneum. In addition, this is the point in the manufacturing process where there is a complete change in media formulation. As such, the high Ki67 staining seen at day 16 in keratinocytes may be the result of the cells responding to different media components. Ki67 staining of Day 20 constructs confirms the high levels of keratinocyte proliferation observed in the final BLCC (Figure 2J–L), which indicates that keratinocytes in the final construct are viable and active. A reduction in fibroblast proliferation was observed throughout the manufacture of the BLCC. At Day 20, the fibroblast and epithelial layers from $n = 4$ BLCCs were physically separated, and the fibroblast matrix was enzymatically digested to release the cells. Figure 2H shows that approximately 10 million fibroblasts were yielded from the final product, and that greater than 95% of these fibroblasts had intact cell membranes, which is an indication of cell viability.

Maximum tensile load

The maximum tensile load of each construct is shown in Figure 4. BLCC supported significantly more load than either the Fibroblast matrix or the Epithelium only constructs ($p < 0.05$, $n = 3$). We hypothesize that the greatest strength imparted to the BLCC construct is due to the formation of a stratified epithelial layer. Additionally, paracrine interaction between fibroblasts and keratinocytes may increase tensile strength of the fibroblast matrix in the BLCC. In the Epithelium only constructs, poor differentiation and lack of a properly formed stratum corneum resulted in tensile strength which was not statistically different than the Fibroblast matrix. Only the combination of fibroblasts and keratinocytes in the BLCC promoted formation of a differentiated epithelium, likely due to the intact basement membrane formed, yielding an increased maximum tensile load in the BLCC compared with Fibroblast matrix or Epithelium only constructs.

Gene expression analysis

Differential expression of genes was observed between the BLCC, Fibroblast matrix, and Epithelium only constructs. In
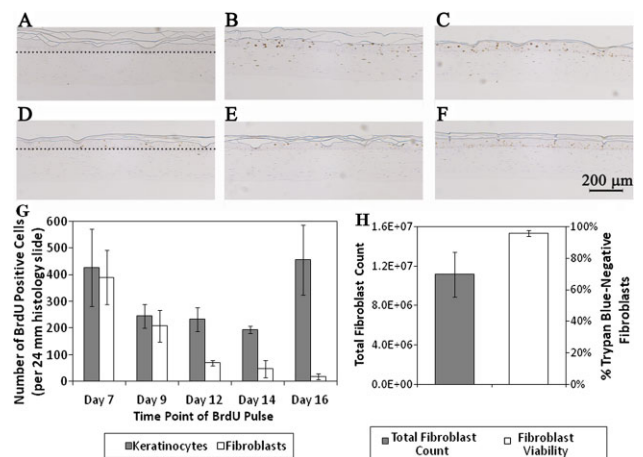

Figure 3. BrdU staining identifies proliferating cells in the BLCC throughout the culture process. BLCC medium remained unmodified (non-BrdU pulsed negative control) (A), or was pulsed with BrdU at Day 7 (B), Day 9 (C), Day 12 (D), Day 14 (E), or Day 16 (F), which was 12 hours prior to the scheduled media change. The scale bar in (F) represents 200 μm for (A), (B), (C), (D), (E), and (F). Dotted lines in (A) and (D) demarcate the epithelium–matrix interface. BrdU positive cells are stained brown. Images are representative of $n = 3$ constructs at each time point. Keratinocyte proliferation remained high up to Day 16, while fibroblast proliferation decreased over time (G). Proliferation was quantified (G) by counting the total number of BrdU-positive keratinocytes and fibroblasts per 24 mm biopsy sample ($n = 3$ samples per time point). Total fibroblast yield and viability were assessed at Day 20 (H) by collagenase digestion of the fibroblast matrix of the BLCC and trypan blue exclusion ($n = 4$). Data in (G) and (H) are presented as mean ± SD, $n = 4$. BLCC, bilayered living cellular construct; BrdU, bromodeoxyuridine.
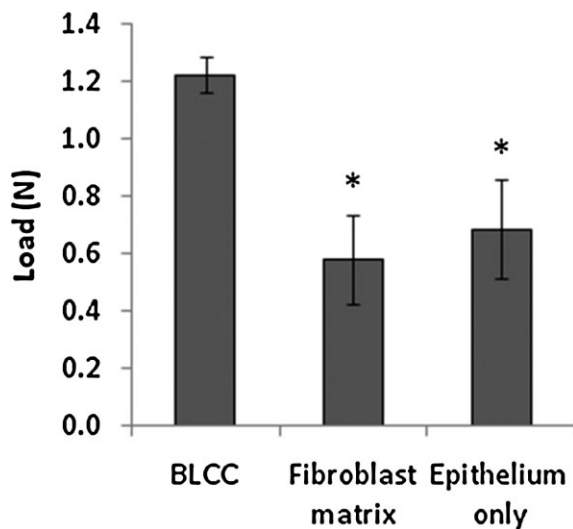
Figure 4. BLCC shows greater maximum tensile load compared with Fibroblast matrix or Epithelium only. Tensile strength is imparted by the properly formed corneal layer, which was present in BLCC but not Fibroblast matrix or Epithelium only constructs. BLCC supported significantly greater maximum tensile load than Fibroblast matrix or Epithelium only constructs. *Indicates different from BLCC ($p < 0.05$, ANOVA). Data are presented as mean ± SD, $n = 3$. BLCC, bilayered living cellular construct.

total, 50 genes were up-regulated in the BLCC compared with the Fibroblast matrix construct, while 19 genes were down-regulated. In comparison with the Epithelium only group, nine genes were up-regulated in the BLCC while 51 genes were down-regulated (Figure 5A). Selected genes were categorized into five key areas of wound healing based on functions commonly described in literature: angiogenesis, cell recruitment, cell growth and differentiation, inflammation, and cell proliferation (Figure 5B). Gene expression between the BLCC, Fibroblast matrix, and Epithelium only also dif-

fered for these particular genes. The results showed that the presence of both fibroblasts and keratinocytes in the BLCC construct modulated gene expression compared with constructs containing either cell type alone.

Cytokine and growth factor production

The analysis of cytokine and growth factor concentration in conditioned medium collected during the manufacturing process showed differences between the constructs. Interestingly, each construct type produced significantly different levels of IL6 and IL8 ($p < 0.05$, Kruskal–Wallis pairwise comparisons, $n = 4$), except for Fibroblast matrix and BLCC at Day 6, which corresponds to the time point when these two constructs have identical composition (i.e., fibroblasts cultured in a collagen matrix for 6 days) (Figure 6A and B). Furthermore, BLCC and Epithelium only were not significantly different at Day 10 for IL8 (Figure 6B). At Day 8, BLCC produced synergistically higher levels of IL6 and IL8 compared with Fibroblast matrix or Epithelium only constructs (Figure 6A and B), which is likely due to the proliferation of keratinocytes taking place at this stage in the process. This synergy was also present for IL6 at Days 10, 13, and 15 (Figure 6A). For VEGF, BLCC produced a significantly greater concentration of VEGF compared with either the Fibroblast matrix or the Epithelium only constructs at Days 15, 17, and 20 (Figure 6C, $p < 0.05$, ANOVA, $n = 4$). Importantly, the VEGF production from the BLCC increased synergistically compared with constructs containing only one cell type. At Day 20, the concentration of IGF-1 in conditioned media was greater for the Fibroblast matrix construct compared with the Epithelium only construct and the BLCC (Figure 7A, $p < 0.05$, Kruskal–Wallis, $n = 3$). Conversely, BMP-2 was detected at Day 20 in conditioned media from all constructs but was not significantly different between the BLCC, Fibroblast matrix, and Epithelium only constructs (Figure 7B, ANOVA). Taken together, these observations provide support that selective cross talk occurs between fibroblasts and keratinocytes in the BLCC, which changes the production of certain cytokine/growth factors in the BLCC compared with constructs containing only one cell type.
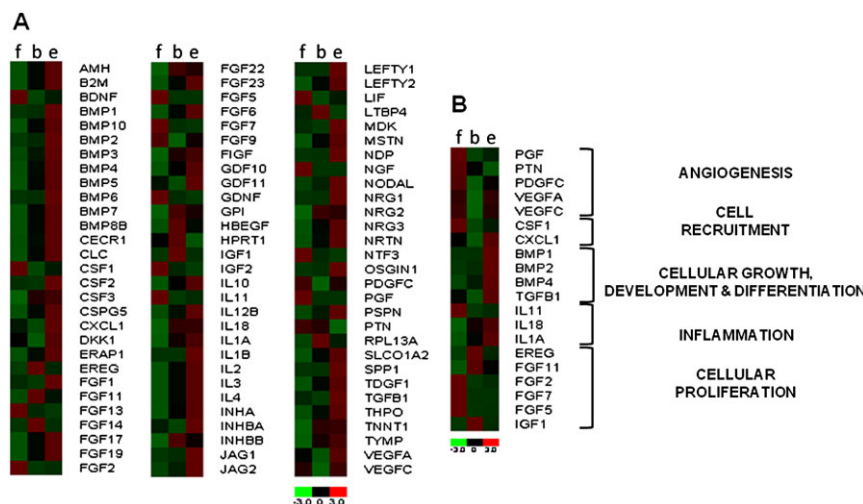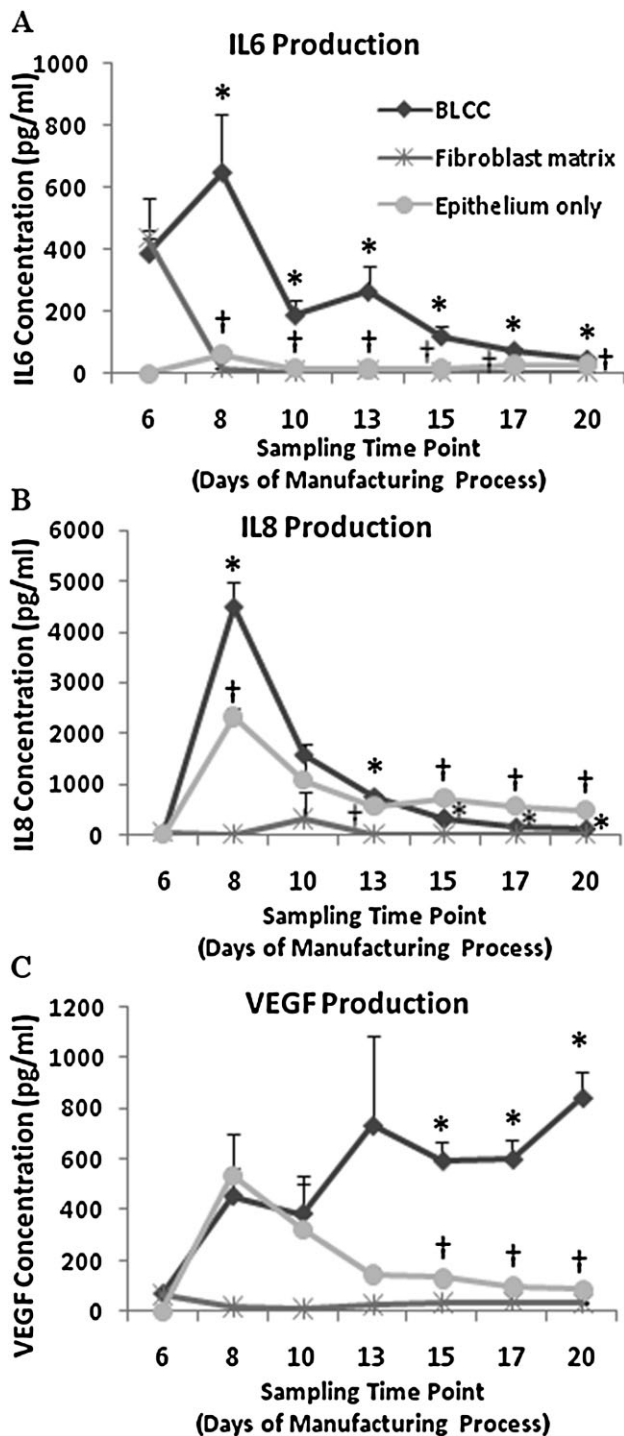

Figure 5. Gene expression varies between Fibroblast matrix (f), BLCC (b), and Epithelium only (e). The heat map shows relative gene expression of the experimental groups (*x*-axis) normalized to GAPDH and β-actin housekeeping genes. The full growth factor array is shown in (A), while a subset of wound healing genes is highlighted in (B). BLCC, bilayered living cellular construct.

A

IL6 Production

B

IL8 Production

C

VEGF Production

Figure 6. The concentration of cytokines and growth factors in the BLCC conditioned medium differs from Fibroblast matrix or Epithelium only conditioned media throughout the manufacturing process. IL-6 (A), IL-8 (B), and VEGF (C) concentrations in conditioned media were quantified at each time point in the manufacturing process. Each construct produced significantly different levels of IL6 and IL8 compared with the other two constructs within the same time point ($p < 0.05$, Kruskall–Wallis, $n = 4$), except at Day 6, in which BLCC and Fibroblast matrix were not different. For VEGF, each construct produced significantly different levels of VEGF compared with the other two constructs at Days 15, 17, and 20 ($p < 0.05$, ANOVA, $n = 4$). *Indicates different from Fibroblast matrix and Epithelium only within same time point ($p < 0.05$). †Indicates different from Fibroblast matrix within same time point ($p < 0.05$). Data are presented as mean ± SD, $n = 4$ constructs per time point. BLCC, bilayered living cellular construct; IL, interleukin; VEGF, vascular endothelial growth factor.

was used to quantify the total network length, number of branching points, and total loops. An example of output images generated by the software is provided in Figure 8M–P, and these images were generated from the input images shown in Figure 8I–L. Conditioned media from BLCC and Epithelium only constructs were not significantly different in terms of the total network length maintained on the Matrigel at any time point in the study. However, these groups promoted significantly more network maintenance than the Fibroblast matrix, as measured by total network length (Figure 8Q). Surprisingly, the BLCC and Epithelium only conditioned media also outperformed the EGM positive control media ($p < 0.05$, ANOVA, $n = 3$). No differences were noted in branching points at Day 2 due to high variability in the data; however, by Day 6 BLCC maintained significantly greater branch points than either Fibroblast matrix or Epithelium only (Figure 8R, $p < 0.05$, Kruskal–Wallis). Furthermore, BLCC and Epithelium only maintained significantly more total loops at Days 2 and 6 compared with Fibroblast matrix (Figure 8S, $p < 0.05$, Kruskal–Wallis). Taken together, these data show that the conditioned medium from the Fibroblast matrix does not support network formation in vitro, while medium from Epithelium only and BLCC supports network formation and maintenance. It is important to point that hUVECs were used in this assay rather than microvascular endothelial cells, those commonly found in skin. Thus, it is possible that the responses may have been different. Nevertheless, in the context of this study, the results indicate that keratinocytes may impart angiogenic properties to the BLCC.

DISCUSSION

Bioengineered products are thought to accelerate wound healing through the delivery of matrix proteins and soluble factors and by providing a barrier to moisture loss and bacterial infection. In normal skin, dermal fibroblasts maintain the extracellular matrix, which provides signaling molecules that promote keratinocyte growth and differentiation. Keratinocytes, in turn, stratify to form the epithelial layer, providing mechanical integrity and barrier function for the tissue and signaling to fibroblasts for continued tissue homeostasis. The paracrine signaling between fibroblasts and keratinocytes, known as cross talk, is what maintains normal
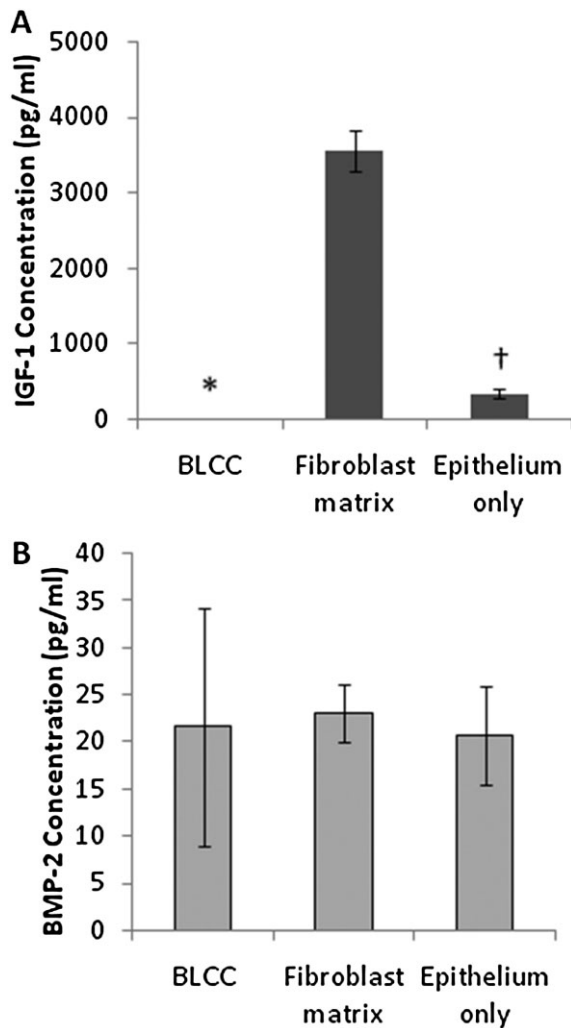
In vitro endothelial network maintenance

The extent of hUVEC network maintenance when cultured with conditioned media from the various constructs was monitored over 6 days using time-lapse microscopy. Representative images of the hUVEC networks from each group at Days 2, 4, and 6 are shown in Figure 8A–L. Wimasis software

Figure 7. Growth factor concentrations produced in conditioned media at Day 20 vary by construct type for IGF-1 (A) but are not different for BMP-2 (B). The Fibroblast matrix produced high levels of IGF-1, which was diminished when combined with keratinocytes in the BLCC. BMP-2 production did not change based on the cell types present in the constructs. For nonnormally distributed IGF-1 data, Kruskal–Wallis with pairwise comparisons was performed. For normally distributed BMP-2 data which exhibited non-homogeneity of variances, ANOVA with Welch correction factor was performed. *Indicates different from Fibroblast matrix and Epithelium only within same time point ($p < 0.05$). †Indicates different from Fibroblast matrix within same time point ($p < 0.05$). Data are presented as mean ± SD, $n = 4$. BLCC, bilayered living cellular construct; IGF-1, insulin-like growth factor-1; BMP-2, bone morphogenetic protein-2.

bioengineered format are required to generate a fully developed epithelium, creating a construct with a unique growth factor and cytokine profile compared with constructs containing only one cell type. Any extrapolation of these findings to other three-dimensional cellular constructs, not incorporating collagen, would require further investigation.

The specific morphology of the BLCC is predicated from cross talk between the two cell types present in the construct. This cross talk may result from direct cellular contact of the two cell types, soluble signaling between the two cell types, or a combination of both. In the current study, the presence of collagen type IV at the dermal–epidermal junction in the BLCC but not the Fibroblast matrix or the Epithelium only constructs confirms the need for both keratinocytes and fibroblasts to induce basement membrane deposition. Basement membrane deposition ensures adherence between the dermal
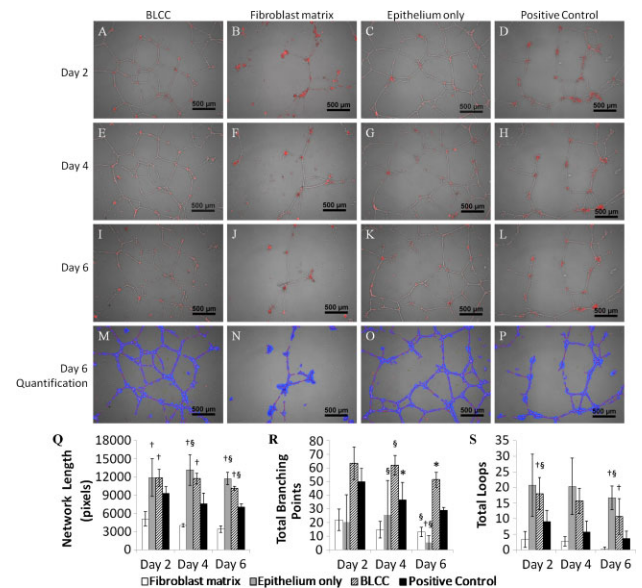

Figure 8. BLCC and Epithelium only conditioned media promoted hUVEC network maintenance over the course of 6 days. Representative images at 5× magnification of hUVEC networks at Day 2 (A–D), Day 4 (E–H), and Day 6 (I–L) after application of conditioned media to preformed hUVEC networks on Matrigel show degradation (Fibroblast matrix) or maintenance (BLCC and Epithelium only) of the networks over time. Each image in A–L is a representative of $n = 3$ biological replicates and is a merge of phase contrast and fluorescence. Images were quantified using Wimasis software, and the output images from I–L are shown in M–P. Total network length (Q), total braching points (R), and total loops (S) are shown for each condition at all time points. For normally distributed tube length data, ANOVA with post hoc Tukey was performed. For nonnormally distributed branch point and total loop data, Kruskal–Wallis with pairwise mean rank comparisons was performed. *Indicates different from Fibroblast matrix and Epithelium only within same time point ($p < 0.05$). †Indicates different from Fibroblast matrix within same time point ($p < 0.05$). §Indicates different from Positive Control. Data are presented as mean ± SD, $n = 3$. BLCC, bilayered living cellular construct; hUVEC, human umbilical vein endothelial cell.

tissue function and is essential for restoring tissue homeostasis in wound healing.[10,11,23] Although bioengineered skin constructs with two cell types do not fully recapitulate the entire structure and function of native human skin,[24–26] the current study shows that both keratinocytes and fibroblasts in a

and epidermal layers of the construct and increases the mechanical strength of the tissue.[27,28] Furthermore, establishment of the basement membrane stimulates the development of a well-stratified epithelium, including the *stratum corneum*, which imparts a barrier function to the BLCC.[29] Our unpublished work has shown that there is a targeted amount of fibroblasts required to ensure basement membrane deposition, leading to a stratified epithelium, equivalent to the dose that was used in this study. Additionally, increasing the fibroblast density by twofold did not change the overall deposition of basement membrane, as assessed qualitatively by collagen type IV staining. Cytokeratin 1/10 staining showed the presence of differentiated keratinocytes in the stratified layers of the BLCC, while this stratification was absent in the Fibroblast matrix and Epithelium only constructs. These results are consistent with other studies using a similar test model,[30–32] showing the necessity of both cell types for proper epidermal stratification.

It is known that keratinocyte stem cells reside in the basal layer of the skin epidermis. In the current study, proliferating cells in the Day 20 BLCC were primarily located in the basal cell layer of the epithelium, while Day 20 Fibroblast matrix and Epithelium only constructs did not contain proliferating cells. Carlson et al. demonstrated that a subset of keratinocytes in BLCC are keratinocyte stem cells due to their ability to maintain colony-forming efficiency in vitro, produce clonal epidermal units in vivo, and retain the ability to recapitulate a stratified epithelium multiple times.[33] Previous studies have shown keratinocyte cultures that consist only of transit amplifying cells or differentiated keratinocytes and lack keratinocyte stem cells are unable to form a well-stratified epithelial compartment in vitro, even when cultured in the presence of fibroblasts.[34] Taken together, these results show that the manufacturing process of BLCC maintained a robust source of keratinocyte stem cells that were able to construct a properly stratified epidermis in the presence of fibroblasts.

Growth factor-mediated cross talk between keratinocytes and fibroblasts plays a central role in wound healing.[10,11] Previous studies have shown that the BLCC produces a broad range of cytokines and growth factors.[35,36] This study showed that the BLCC had a unique gene expression profile compared with either the Fibroblast matrix or Epithelium only constructs. Differential expression of genes, such as *BMP*s, *EREG*, *FGF11*, *IGF1*, *PDGF*, and *VEGF*, among the three constructs, shows that the presence of both fibroblasts and keratinocytes in BLCC alters the gene expression profile. Similarly, cytokine and growth factor concentrations in conditioned media were modulated by coculture of fibroblasts and keratinocytes in BLCC. BLCC produced a unique profile of IL-6, IL-8, VEGF, and IGF-1 compared with either single cell type construct. In regard to wound healing, IL-6 can act as both a pro-inflammatory and anti-inflammatory cytokine, and has a proliferative effect on keratinocytes.[9,37] IL-8 is a major mediator of inflammatory response due to its role as a chemoattractant of neutrophils,[9] and it is also a potent angiogenic factor.[38] VEGF is important in stimulating angiogenesis, a process that is central to tissue regeneration.[39] IGF-1 is expressed by fibroblasts and promotes keratinocyte proliferation.[12] In contrast, BMP-2, which has been observed in skin[40] and promotes a differentiated keratinocyte phenotype,[41,42] was not significantly different among the three constructs, indicating that cross talk does not modulate every protein produced by BLCC. Further study of a broader array of genes and

proteins, including IL-1α, IL-1β, and KGF, for example, is warranted. However, the coculture of keratinocytes and fibroblasts within BLCC overall produces a unique gene and protein profile compared with one cell type constructs, which is likely the result of cross talk between the two cell types.

In the context of wound healing, angiogenesis is essential for the support of provisional matrices within the wound as well as repair of healthy skin tissue.[5,9] The results from this study showed that fibroblasts and keratinocytes within the BLCC produce soluble factors that support formation and maintenance of in vitro endothelial networks. These data suggest that BLCC has angiogenic properties, which may be important in the wound environment.

In conclusion, this study characterizes BLCC, a commercially available product for the treatment of DFUs and VLUs. BLCC in this study was produced using the same process as that employed in large-scale fabrication. Therefore, the properties described herein can be applied to the large-scale product. These results provide evidence that fibroblasts and keratinocytes within BLCC are involved in active cross talk that imparts structural, mechanical, and biochemical properties to the construct that are not present in constructs containing only one cell type. BLCC has a well-stratified epithelium, which imparts mechanical integrity to the construct, and contains metabolically active keratinocyte stem cells, which are important in wound healing. Gene expression and protein production are modulated by the presence of both cell types in the BLCC. This modulation may be specific to genes and proteins relevant to skin homeostasis and wound healing; however, further characterization of a broader array of growth factors and cytokines is necessary. Finally, BLCC conditioned medium promoted formation of endothelial cell networks, and this in vitro angiogenic effect was paracrine in nature. The in vitro results described in this paper will be translated into an appropriate preclinical animal model in future studies to understand the importance of cross talk in the wound healing process. In summary, the cross talk provided by the presence of both fibroblasts and keratinocytes within a bilayered living cellular construct imparts unique properties to the construct which are important for tissue homeostasis and wound healing.

REFERENCES

1. Martin P. Wound healing—aiming for perfect skin regeneration. *Science* 1997; 276: 75–81.
2. Shaw TJ, Martin P. Wound repair at a glance. *J Cell Sci* 2009; 122 (Pt 18): 3209–13.
3. Singer AJ, Clark RA. Cutaneous wound healing. *N Engl J Med* 1999; 341: 738–46.
4. Willenborg S, Knipper J, Ranjan R, Krieg T, Eming S. Chronic wounds and inflammation. In: Sen C, DePietro L, Roy S, editors.

Advances in wound care. New Rochelle, NY: Mary Ann Liebert, Inc, 2010: 259–65.

5. Schultz GS, Davidson JM, Kirsner RS, Bornstein P, Herman IM. Dynamic reciprocity in the wound microenvironment. *Wound Repair Regen* 2011; 19: 134–48.

6. Valencia IC, Falabella A, Kirsner RS, Eaglstein WH. Chronic venous insufficiency and venous leg ulceration. *J Am Acad Dermatol* 2001; 44: 401–21.

7. Driver VR, Fabbi M, Lavery LA, Gibbons G. The costs of diabetic foot: the economic case for the limb salvage team. *J Am Podiatr Med Assoc* 2010; 100: 335–41.

8. Centers for Disease Control. *National diabetes fact sheet: national estimates and general information on diabetes and prediabetes in the United States*. 2011. Ref Type: Pamphlet.

9. Barrientos S, Stojadinovic O, Golinko MS, Brem H, Tomic-Canic M. Growth factors and cytokines in wound healing. *Wound Repair Regen* 2008; 16: 585–601.

10. Tomic-Canic M. Keratinocyte cross-talks in wounds. *Wounds* 2005; 17: S3–6.

11. Werner S, Krieg T, Smola H. Keratinocyte-fibroblast interactions in wound healing. *J Invest Dermatol* 2007; 127: 998–1008.

12. Shirakata Y. Regulation of epidermal keratinocytes by growth factors. *J Dermatol Sci* 2010; 59: 73–80.

13. Edmondson SR, Thumiger SP, Werther GA, Wraight CJ. Epidermal homeostasis: the role of the growth hormone and insulin-like growth factor systems. *Endocr Rev* 2003; 24: 737–64.

14. Heng MC. Wound healing in adult skin: aiming for perfect regeneration. *Int J Dermatol* 2011; 50: 1058–66.

15. Maas-Szabowski N, Szabowski A, Stark HJ, Andrecht S, Kolbus A, Schorpp-Kistner M, et al. Organotypic cocultures with genetically modified mouse fibroblasts as a tool to dissect molecular mechanisms regulating keratinocyte growth and differentiation. *J Invest Dermatol* 2001; 116: 816–20.

16. Bao P, Kodra A, Tomic-Canic M, Golinko MS, Ehrlich HP, Brem H. The role of vascular endothelial growth factor in wound healing. *J Surg Res* 2009; 153: 347–58.

17. Auger FA, Lacroix D, Germain L. Skin substitutes and wound healing. *Skin Pharmacol Physiol* 2009; 22: 94–102.

18. Veves A, Falanga V, Armstrong DG, Sabolinski ML. Graftskin, a human skin equivalent, is effective in the management of noninfected neuropathic diabetic foot ulcers: a prospective randomized multicenter clinical trial. *Diabetes Care* 2001; 24: 290–5.

19. Falanga V, Margolis D, Alvarez O, Auletta M, Maggiacomo F, Altman M, et al. Rapid healing of venous ulcers and lack of clinical rejection with an allogeneic cultured human skin equivalent. Human Skin Equivalent Investigators Group. *Arch Dermatol* 1998; 134: 293–300.

20. Parenteau N. Skin equivalents. In: Leigh I, Watt F, editors. *Keratinocyte methods*. Cambridge: Cambridge University Press, 1994: 45–55.

21. Wilkins LM, Watson SR, Prosky SJ, Meunier SF, Parenteau NL. Development of a bilayered living skin construct for clinical applications. *Biotechnol Bioeng* 1994; 43: 747–56.

22. Li C, Wong WH. Model-based analysis of oligonucleotide arrays: expression index computation and outlier detection. *Proc Natl Acad Sci U S A* 2001; 98: 31–6.

23. Werner S, Smola H. Paracrine regulation of keratinocyte proliferation and differentiation. *Trends Cell Biol* 2001; 11: 143–6.

24. Boyce ST, Supp AP, Swope VB, Warden GD. Vitamin C regulates keratinocyte viability, epidermal barrier, and basement membrane in vitro, and reduces wound contraction after grafting of cultured skin substitutes. *J Invest Dermatol* 2002; 118: 565–72.

25. Smiley AK, Klingenberg JM, Aronow BJ, Boyce ST, Kitzmiller WJ, Supp DM. Microarray analysis of gene expression in cultured skin substitutes compared with native human skin. *J Invest Dermatol* 2005; 125: 1286–301.

26. Klingenberg JM, McFarland KL, Friedman AJ, Boyce ST, Aronow BJ, Supp DM. Engineered human skin substitutes undergo large-scale genomic reprogramming and normal skin-like maturation after transplantation to athymic mice. *J Invest Dermatol* 2010; 130: 587–601.

27. Chan LS. Human skin basement membrane in health and in autoimmune diseases. *Front Biosci* 1997; 2: d343–52.

28. Ko MS, Marinkovich MP. Role of dermal-epidermal basement membrane zone in skin, cancer, and developmental disorders. *Dermatol Clin* 2010; 28: 1–16.

29. Parenteau N, Sabolinski M, Prosky S, Nolte C, Oleson M, Kriwet K, et al. Biological and physical factors influencing the successful engraftment of a cultured human skin substitute. *Biotechnol Bioeng* 1996; 52: 3–14.

30. Marionnet C, Pierrard C, Vioux-Chagnoleau C, Sok J, Asselineau D, Bernerd F. Interactions between fibroblasts and keratinocytes in morphogenesis of dermal epidermal junction in a model of reconstructed skin. *J Invest Dermatol* 2006; 126: 971–9.

31. Andriani F, Margulis A, Lin N, Griffey S, Garlick JA. Analysis of microenvironmental factors contributing to basement membrane assembly and normalized epidermal phenotype. *J Invest Dermatol* 2003; 120: 923–31.

32. Erdag G, Sheridan RL. Fibroblasts improve performance of cultured composite skin substitutes on athymic mice. *Burns* 2004; 30: 322–8.

33. Carlson M, Faria K, Shamis Y, Leman J, Ronfard V, Garlick J. Epidermal stem cells are preserved during commercial-scale manufacture of a bilayered, living cellular construct (Apligraf(R). *Tissue Engin Part A* 2011; 17: 487–93.

34. Li A, Pouliot N, Redvers R, Kaur P. Extensive tissue-regenerative capacity of neonatal human keratinocyte stem cells and their progeny. *J Clin Invest* 2004; 113: 390–400.

35. Falanga V, Butmarc J, Cha J, Yufit T, Carson P. Migration of the epidermal over the dermal component (epiboly) in a bilayered bioengineered skin construct. *Tissue Eng* 2007; 13: 21–8.

36. Brem H, Young J, Tomic-Canic M, Isaacs C, Ehrlich HP. Clinical efficacy and mechanism of bilayered living human skin equivalent (HSE) in treatment of diabetic foot ulcers. *Surg Technol Int* 2003; 11: 23–31.

37. Akira S, Hirano T, Taga T, Kishimoto T. Biology of multifunctional cytokines: IL 6 and related molecules (IL 1 and TNF). *FASEB J* 1990; 4: 2860–7.

38. Li A, Dubey S, Varney ML, Dave BJ, Singh RK. IL-8 directly enhanced endothelial cell survival, proliferation, and matrix metalloproteinases production and regulated angiogenesis. *J Immunol* 2003; 170: 3369–76.

39. Ng YS, Krilleke D, Shima DT. VEGF function in vascular pathogenesis. *Exp Cell Res* 2006; 312: 527–37.

40. Hogan BL. Bone morphogenetic proteins: multifunctional regulators of vertebrate development. *Genes Dev* 1996; 10: 1580–94.

41. Botchkarev VA. Bone morphogenetic proteins and their antagonists in skin and hair follicle biology. *J Invest Dermatol* 2003; 120: 36–47.

42. Gosselet FP, Magnaldo T, Culerrier RM, Sarasin A, Ehrhart JC. BMP2 and BMP6 control p57(Kip2) expression and cell growth arrest/terminal differentiation in normal primary human epidermal keratinocytes. *Cell Signal* 2007; 19: 731–9.